International Journal of Civil Engineering (2025) 23:1323–1334
https://doi.org/10.1007/s40999-025-01090-4

RESEARCH PAPER

Correlation Between Flexural-Tensile and Direct Shear Behavior of SFRC

Julian Carrillo[1,4] · Nestor Guerrero[2] · Carlos Piscal[3]

Received: 25 April 2024 / Revised: 5 February 2025 / Accepted: 24 February 2025 / Published online: 24 March 2025

Abstract

Correlations between fiber characteristics and the compressive, flexural-tensile, and shear strengths of steel fiber reinforced concrete (SFRC) are proposed in the literature to facilitate the code-compliant design. In this study, the correlation between flexural-tensile and direct shear stresses on plain concrete (PC) and SFRC beams and columns is evaluated. The database included 1767 data from direct shear tests of beam and column, and from four-point bending tests (4PBT) of PC and SFRC beams. Data comprised measured results from this study and from the results of other research programs published in the literature. The main characteristics of the database were fiber aspect ratios (l_f/d_f between 65 and 80), fiber volume fraction (V_f between 0.25% and 2%), and compressive strength of concrete (f'_c between 28 and 78 MPa). From the trends observed in the experimental results, an empirical equation is proposed to estimate the direct shear and flexural-tensile performance of SFRC. The results of the statistical analysis showed that the equation is a suitable tool to estimate the maximum direct shear and flexural-tensile strengths of SFRC. The correlation between shear and flexural-tensile strengths would facilitate SFRC code-compliant design.

Keywords Fiber-reinforced concrete · Steel fibers · Direct shear · Flexural-tensile · Four-point bending test · Residual strength

1 Introduction

Shear failure in concrete structures is a sudden and catastrophic mode of failure [1]. One of the most promising options for reinforcing structural elements are steel fibers. Previous studies have shown the effectiveness of fibers in improving different mechanical properties of concrete, particularly the tensile, bending and shear strengths of plain concrete (PC) [2]. Lozano [3], for instance, studied the use of SFRC in deep beams with fiber volume fraction (V_f) of 1% and 2% and found that factors such as the type of fiber, aspect ratio (l_f/d_f), V_f and type of concrete influence the shear strength of these elements. Lozano [3] concluded that shear transfer in SFRC elements derives mainly from the tensile and compressive strength of concrete. For example, Lozano [3] argued that steel fibers improve the tensile residual stress transferred through the cracks in deep beams because the flexural strength of concrete with V_f of 1.5% can increase up to 150%. Sarta and Silva [4] also demonstrated that flexural strength of SFRC beams with V_f of 4% and 6% increased by 45% and 56%, respectively, when compared to PC. In terms of aspect ratio of fibers, Marmol [5] observed that the greatest flexural capacity is obtained when using a lower value of l_f/d_f due to the increased number of fibers present in the concrete matrix helping to join the cracks. Barragán et al. [6] argued that the use of steel fibers as shear reinforcement of concrete aids to

✉ Julian Carrillo
julian.carrillo@unimilitar.edu.co

Nestor Guerrero
nestor.guerrero@unibague.edu.co

Carlos Piscal
carlos@earthquakeprotection.com

[1] Department of Civil Engineering, Universidad Militar Nueva Granada, Bogotá, Colombia

[2] Department of Civil Engineering, Universidad de Ibagué, Ibagué, Colombia

[3] Earthquake Protection System, Bogotá, Colombia

[4] Colombian Earthquake Engineering Research Network, CEER, Bogotá, Colombia

modify the brittle shear failure mode by a mixed shear-flexure mode.

In terms of the shear strength of SFRC, Wu et al. [7] studied the shear behavior of ultra high performance concrete (UHPC) reinforced with V_f of 0.5%, 1.5% and 2.5% of steel fibers using the Z-type test method. These authors argued that steel fibers improve the mechanical integrity of concrete under shear stresses. Wu et al. [7] concluded that the equations prescribed by ACI 318-08 Building Code [8] and the PCI manual [9] fail in predicting accurately the direct shear strength of UHPC. López [1] found that the shear strength of SFRC with V_f of 0.5% is 7% higher than that of PC, and that the increment is 30% and 55% for SFRC with V_f of 0.76% and 1.0%, respectively. Barragán et al. [6] studied the shear failure of SFRC based on the Z-type push-off tests with fiber dosages (D_f) of 0, 20 and 40 kg/m^3. They found that the cracks appearing during the shear test may result not only in a decreased peak shear strength but also in the specimens failing due to a mixed shear-flexural mode [6]. Khanlou et al. [10] studied the shear performance of SFRC with D_f of 20, 40, 60, and 80 kg/m^3 and found that the failure mode of the beam changes from brittle to ductile failure when the steel fiber dosage D_f is higher than 20 kg/m^3. Araujo et al. [11], in turn, studied the shear strength of SFRC beams with V_f of 1% and 2%, and found that steel fibers are effective to increase the shear strength of concrete. They noted that the shear strength of concrete increased in 87% and 99% when adding steel fibers with V_f of 1% and 2%, respectively [9]. Araujo et al. [11] also observed that after maximum shear loading, the load abruptly decreases by approximately 60% and 50% with V_f of 1% and 2%, respectively.

Results of previous studies confirm that steel fibers are a reinforcement alternative for concrete elements such as slabs, beams, columns, and walls. The increasing use of this material requires tools to correlate the performance of SFRC under an easily obtained flexural-tensile stress and that under direct shear stress, which is difficult to determine experimentally. Establishing such numerical correlations between the mechanical properties of SFRC under simplified and complex loading conditions are also essential to facilitate the process of code-compliant design. Carrillo et al. [12, 13] developed models to correlate the tensile performance of concrete reinforced with hooked-end steel fibers using four-point bending tests (4PBT) with that using three-point bending tests (3PBT) and double punch tests (DPT). The present study evaluated the performance of SFRC under flexural-tensile and direct shear stresses. The study included three direct shear test methods to adequately evaluate the correlation between direct shear stress of beams and columns, and flexural-tensile stress of beams. The test methods used to evaluate shear strength of PC and SFRC were the Z-type method [1], the standard method of the Japanese Society of Civil Engineering JSCE-SF6 [14], and the standard shear test of the International Federation of Prestressing (FIP) [15]. Shear stress at cracking and maximum limit states, and three residual shear stresses were determined during testing. The flexural-tensile strength of SFRC was evaluated according to the four-point beam test (4PBT) established by the ASTM C1609 American standard [16], since this is a commonly used standard in the literature to determine flexural-tensile performance of SFRC. Compressive strength, modulus of elasticity, and Poisson's ratio of the PC and SFRC were also experimentally assessed. Slump, unit mass and fiber dosage of fresh concrete were measured to evaluate the fresh state of the PC and the SFRC. In this study, a numerical correlation is proposed to estimate the basic properties of SFRC under bending and direct shear stresses of SFRC. The correlation models were developed between shear and flexural-tensile strengths through the trends of shear strengths as a function of flexural-tensile stresses. An analysis of variance (ANOVA) was carried out to identify the variables that significantly influence the correlation between direct shear and flexural-tensile stresses. Models were calibrated by using 1,767 data from beam and column direct shear tests and flexural-tensile tests of PC and SFRC beams tested in this study and those reported by previous research programs.

2 Experimental Program and Description of the Database

2.1 Description of the Variables and Characteristics of the Specimens

Direct shear tests on beams and columns, and four-point bending tests (4PBT) on PC and SFRC beams were conducted in the present study. The database included 1767 data from 52 tests: 31 are direct shear tests and 21 are 4PBT. Nineteen of the 52 tests were conducted in the present study, while the other 33 correspond to tests reported in studies available in the literature. Fourteen of the 19 tests from the present study were direct shear tests on beam and column specimens tested using the JSCE-SF6 method [14] (6 beam specimens), the FIP method [15] (4 beam specimens), and Z-type method [1] (4 column specimens); and 5 were 4PBT of beam specimens tested according to the ASTM C-1609 standard [16]. Results of previous studies confirmed that the mechanical properties of SFRC depend on fiber content (V_f), aspect ratio of the fiber (l_f/d_f), and compressive strength of concrete (f'_c). Therefore, the variables used were compressive strength of concrete (f'_c between 28 and 78 MPa), fiber content (V_f between 0.3% and 2.0%), and aspect ratio (l_f/d_f between 65 and 80) of steel fibers. According to the ASTM C-1609 standard [12], the following parameters were studied: flexural strength at first cracking (f_{cr}), maximum flexural-tensile strength (f_{max}), and the flexural-tensile residual stresses associated with deflections of 0.75 mm ($f_{L/600}$), 1.5 mm ($f_{L/300}$) and 3 mm ($f_{L/150}$). For direct shear tests, the parameters studied were shear strength at first cracking (τ_{cr}), maximum shear strength (τ_{max}), and three shear residual stresses (τ_{n120}, τ_{n100}, τ_{n80}).

2.2 Geometry of Specimens and Reinforcement of Specimens

As previously explained, three test methods were used in this study to assess the direct shear strength of concrete: JSCE-SF6, FIP standard and Z-type methods. The dimensions of PC and SFRC beams and columns subjected to direct shear tests depend on the test method. Width and length of beams for JSCE-SF6 and FIP standard methods were: 150 mm and 600 mm, and 250 mm and 540 mm, respectively. Width and length of columns tested using the Z-type method were 200 mm and 440 mm, respectively. Twelve SFRC specimens were constructed; eight beams for the JSCE-SF6 and FIP standard methods, and four columns for the Z-type method. Two PC beams were also constructed for characterizing the direct shear strength of PC using the JSCE-SF6 method.

Khanlou et al. [10] pointed out that notches must be made in beams subjected to direct shear tests to induce failure on specific failure planes. The dimension of the notch is equivalent to 1/10 of the height of the test specimen. Test methods have different numbers of shear planes (N_p). The FIP and Z-type methods define one shear plane, while the JSCE-SF6 method requires two shear planes. In terms of bending tests, width and length of PC and SFRC beams were 150 mm and 600 mm, respectively. The study also comprised compression tests on 9 cylinders to determine the mechanical properties in compression; 3 of the cylinders were made of PC and 6 cylinders were made of SFRC. Diameter and heigh of the cylinders mere 150 mm and 300 mm, respectively, and they were tested according to the ASTM C-39 standard [17].

2.3 Test Setups

2.3.1 Direct Shear Test Setup

Figure 1 shows the setup of the direct shear tests that were carried out in the study. Rollers were used to apply the loads during the FIP and JSCE-SF6 direct shear tests. In Z-type tests, plates were used to apply continuous loads. Linear variable differential transducers (LVDTs) with a capacity of 25 mm were used in the direct shear tests to measure the longitudinal and transverse displacements. Figure 1b shows the transverse LVDTs that were used to determine the crack width in the FIP method. A displacement-controlled rate of 0.007 mm/s was used during the three direct shear test methods. Carmona and Cabrera [19] recommended Eq. (1) to estimate the direct shear strength of the SFRC.

$$\tau_{max} = \frac{P_{max}}{N_p \times b \times h'} \tag{1}$$

where τ_{max} is the maximum shear strength (MPa), P_{max} is the maximum load recorded during the test (N), N_p is the number of shear planes, and h' and b correspond to the effective height and width of the area under load (mm).

Five shear stresses were identified in the direct shear tests to conduct a correlation analysis with the flexural-tensile stresses. Shear stress at cracking (τ_{cr}) and maximum (τ_{max}) limit states, and three residual shear stresses (τ_n) were determined during testing. Residual stresses were established at three residual displacements (D_n), which were calculated as the ratio of the effective height of the specimen and predefined constants (n) for each type of direct shear test. Displacement D_n is a function of the test method since it depends directly on the specimen's effective height. Carmona and Cabrera [19], and Higashiyama and Banthia [20] tested SFRC beams using the JSCE-SF6 method and used n values of 40, 30 and 10, and 80, 40, 25, 20, 15 and 10, respectively. In the present study, n values of 120, 100 and 80 were used since they fit both the specimen dimensions and values of the residual shear strength measured in direct shear tests.

2.3.2 Bending Test Setup

The ASTM C-1609 standard [16] describes the American flexural test or four-point bending test (4PBT). This test procedure allows assessing the post-cracking performance of SFRC beams. The bending test uses a simply supported beam under two loads located in the middle thirds of the clear span. Figure 2a shows the instrumentation of the 4PBT, which includes two LVDTs to measure deflection at the center of the beams. Figure 2b shows the typical load–deflection curve obtained in the 4PBT test. The ASTM C-1609 standard [16] indicates that flexural-tensile stresses must be calculated at loads associated with the proportional limit or first crack appearance (P_{cr}), maximum load (P_{max}), and loads at deflection of 0.75 mm ($P_{L/600}$), 1.5 mm ($P_{L/300}$), and 3 mm ($P_{L/150}$). Equation (2) is used to calculate flexural-tensile stresses at limit states, where P is the load on N, L is the clear span in mm, while b and d are the width and height in mm, respectively. Bending tests were conducted using a universal test machine with a maximum compressive capacity of 2000 kN. Equation (2) was used to

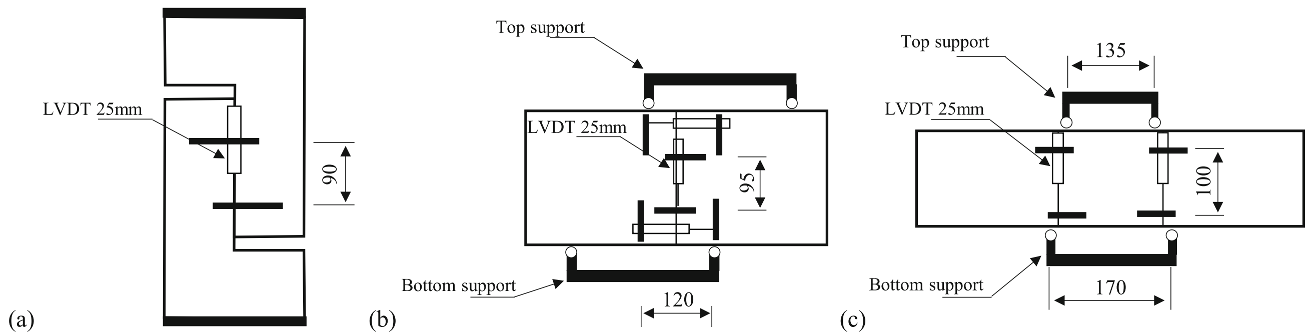

Fig. 1 Direct shear tests setup (dimensions in mm): **a** Z-type, **b** FIP type standard, **c** JSCE-SF6

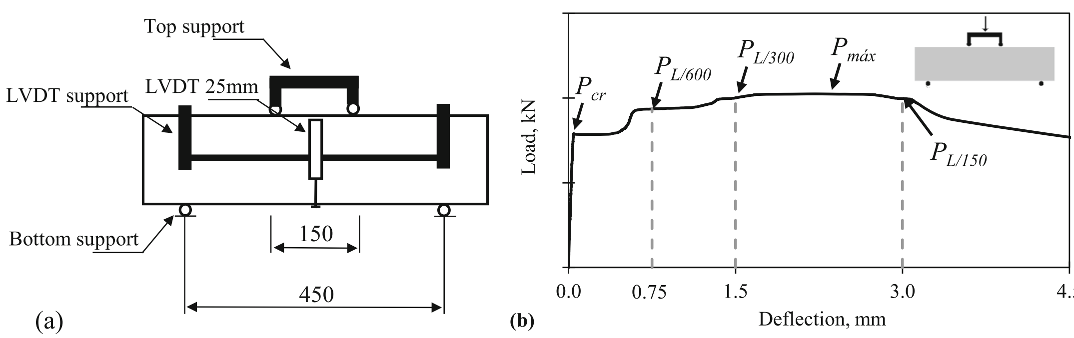

Fig. 2 Four-point bending test—4PBT: **a** setup (dimensions in mm), **b** parameters established by ASTM C-1609 [16]

calculate flexural-tensile stresses (f), where f_{cr} is the first crack flexural strength, f_{max} is the maximum flexural-tensile strength, and $f_{L/600}$, $f_{L/300}$ and $f_{L/150}$ are residual flexural-tensile strengths at deflections of *L/600*, *L/300* and *L/150*, respectively. The ASTM C-1609 standard [16] indicates that the estimated stress must be within a range of beam stresses (f_{max}) from 2.44 MPa to 7.46 MPa.

$$f_b = \frac{P \times L}{b \times d^2} (\text{MPa}) \quad (2)$$

Table 1 Mechanical properties of concrete in fresh state

Property	PC	SFRC-30	SFRC-60
Slump, mm	250	230	180
Unit mass, kg/m^3	2233 (0.8%)	2360 (0.9%)	2321 (1.6%)
$D_{f\text{-}nom}$, kg/m^3	–	30	60
D_f, kg/m^3	–	32.0 (8.9%)	58.1 (12.1%)
$V_{f\text{-}nom}$, %	–	0.38	0.76
V_f, %	–	0.41	0.74
$V_f \times l_f/d_f$	–	26.6	48.1

3 Results and Discussion

3.1 Slump, Unit Mass and Fiber Dosage of Concrete

Table 1 summarizes the average values (X) and the coefficient of variation (CV, in parenthesis) of the test results associated with the fresh state of the PC and the SFRC. As shown in the table, measured dosage (D_f) of steel fibers of specimens tested in this study were of 32.0 and 58.1 kg/m^3. The actual dosages of steel fibers in concrete were determined per EN 14488-7 [18] from the mass of fibers contained in cylinders with a diameter of 150 mm and a height of 300 mm.

3.2 Compression Tests on Cylinders

Figure 3 shows the typical failure modes of specimens tested under compression. As shown in the figure, spalling of concrete is reduced as the fiber dosage (D_f) increases from 32.0 to 58.1 kg/m^3. Markovich et al. [21] and Barragán et al. [6] also reported the bridging effect of steel fibers for closing the cracks due to a more distributed tension stresses on concrete. Table 2 summarizes the average values and the CV (in parenthesis) for the measured compressive strength (f'_c), modulus of elasticity (E_{cf}), and Poisson's ratio (ν) of the PC and SFRC. Values of the measured slump, actual fiber dosage (D_f) and unit mass are included in the table. The values presented in the

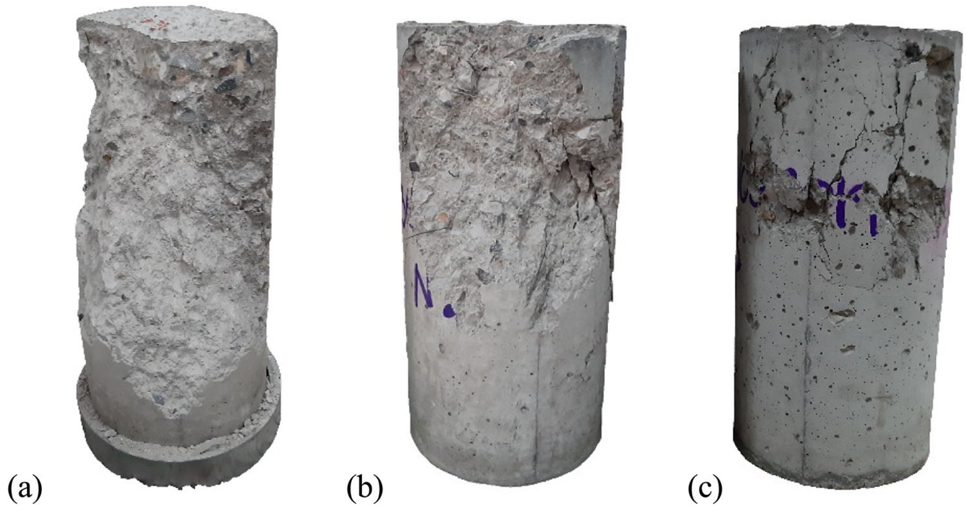

Fig. 3 Typical failure modes of cylinders tested under compression: **a** PC, **b** D_f = 32.0 kg/m^3, **c** D_f = 58.1 kg/m^3

Table 2 Compressive mechanical properties of concrete

Property	PC	SFRC-30	SFRC-60
f'_c, MPa	47.3 (4.0%)	52.7 (2.9%)	52.6 (0.9%)
E_{cf}, MPa	25,172 (1.6%)	26,028 (9.0%)	24,773 (3.5%)
v	0.2 (1.3%)	0.2 (6.4%)	0.2 (19.2%)

table were obtained from three cylinders for each type of test and concrete (PC and SFRC).

Figure 4 shows the compressive stress–strain curves of PC and SFRC specimens with fiber dosage (D_f) of 32.0 kg/m^3 and 58.1 kg/m^3. It can be observed in the figure that the f'_c of SFRC with D_f of 32.0 kg/m^3 (52.7 MPa) and 58.1 kg/m^3 was approximately 11.3% higher than the value of f'_c of PC (47.4 MPa). The difference between the value of f'_c of SFRC with D_f of 32.0 and 58.1 kg/m^3 was lower than 0.2%, so it is considered that the variation of D_f did not affect f'_c. The effect of fibers on the f'_c of SFRC has been previously reported in several studies and it depends on the value of fiber volume fraction (V_f). For V_f values lower than 1%, Lozano [3] pointed out that the effects of SFRC on f'_c are practically non-existent. On the other hand, Sarta and Silva [4] observed that the f'_c of SFRC with V_f of 4% and 6% was 17.3% and 17.5% higher, respectively, than that of the f'_c of PC.

3.3 Direct Shear Tests

Figure 5 shows the typical failure modes of specimens tested under direct shear. Figure 5c, d show an increase in the number of small cracks of SFRC as the dosages increases; for instance, SFRC beams with D_f of 58.1 kg/m^3 and tested using the FIP method exhibited more small cracks close to shear planes than those observed in beams with D_f of 32.0 kg/m^3.

Figure 6 shows the shear stress–displacement curves of the specimens measured during direct shear tests. The scale of the figure was selected to show all the curves at the same figure; however, this scale hinders the option to adequately visualize the curves of plain concrete (PC). Two specimens are shown in Fig. 6 for each D_f in the JSCE-SF6 and FIP methods; in the case of the Z-type method, one specimen is

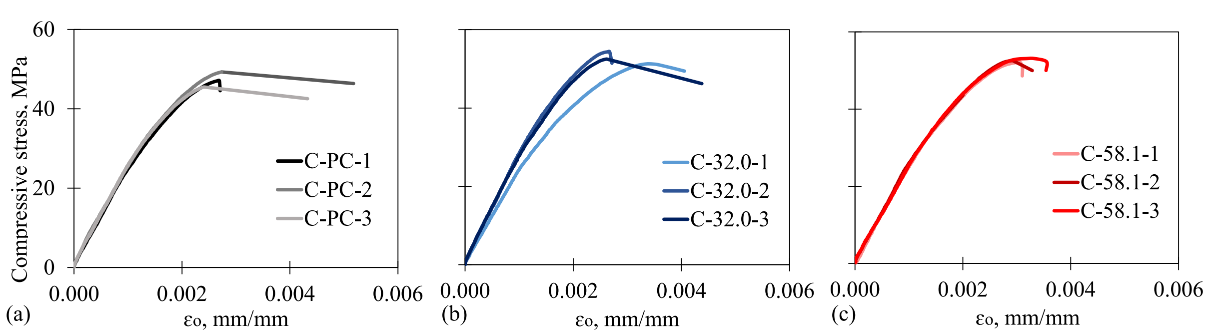

Fig. 4 Compression stress–strain curves: **a** PC, **b** D_f = 32.0 kg/m^3, **c** D_f = 58.1 kg/m^3

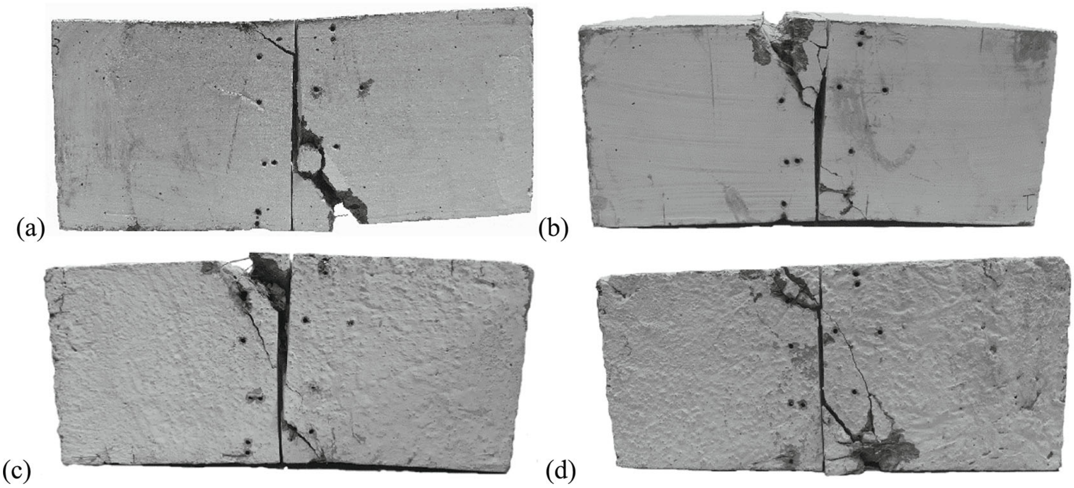

Fig. 5 Typical failure modes of specimens under direct shear tests: **a** FIP-32.0-1, **b** FIP-32.0-2, **c** FIP-58.1-1, **d** FIP-58.1-2

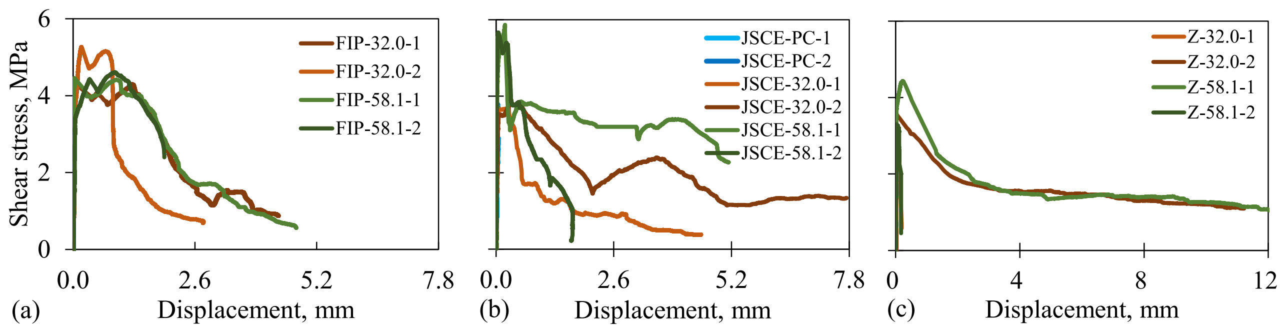

Fig. 6 Shear stress–displacement curves measured during direct shear tests: **a** FIP, **b** JSCE-SF6, **c** Z-type

reported for each D_f, since two specimens failed due to bending and not due to direct shear. Mattock et al. [22] and Higashiyama and Banthia [20] also observed that the failure mode of Z-type specimens can be governed by bending or mixed shear-bending instead of direct shear stresses.

It is observed in Fig. 6 that the maximum shear stress (τ_{max}) in the SFRC specimens occurs after cracking (τ_{cr}), while the τ_{max} of the PC specimens occurs simultaneously with τ_{cr}. The PC specimens only reported τ_{cr} since there is no contribution from the fibers. It is also observed in the figure that τ_{cr} of the specimens with D_f of 58.1 kg/m^3 was 40% at average (between 27.6% and 52.8%) greater than that of specimens with D_f of 32.0 kg/m^3. Yoo et al. [23], Gao et al. [24] and Marmol [5] argued that τ_{cr} of the SFRC depends on the strength of the concrete matrix since the steel fibers are activated after τ_{cr}, which triggers the development of residual shear stresses. As expected and previously reported by Higashiyama and Banthia [20], Fig. 6 shows that the shear strength of the SFRC after τ_{max} decreases as the displacement and the corresponding crack opening increase [25].

Table 3 summarizes values of shear stress at cracking (τ_{cr}) and maximum (τ_{max}) limit states, and three residual shear stresses (τ_n) measured during direct shear tests. Measured values of f'_c and V_f of each specimen is included in the table. The table shows that shear stress at the cracking state (τ_{cr}) of the specimens containing more V_f presents higher shear stresses both at first cracking and maximum shear limit states. An previously explained, increase in the number of small cracks in all specimens tested using the FIP and Z methods of SFRC as the dosages increases was observed. In the present study, the τ_{cr} of SFRC obtained by means of the JSCE-type method with V_f of 0.74% (5.35 MPa) was approximately 53% higher than that of specimens with V_f of 0.41% (3.5 MPa). Yoo et al. [23] pointed out that the τ_{cr} of SFRC depends on the tensile strength of the steel fibers after the first cracking shear strength. In the present study, the τ_{max} of JSCE specimens with V_f of 0.74% (5.65 MPa) was approximately 26% and 28% higher than the τ_{max} strength of FIP-type specimens (4.50 MPa) and Z-type tests (4.40 MPa), respectively.

3.4 Bending Tests on Beams

Figure 7 shows the typical failure modes of specimens under four point bending test (4PBT). Fracture of all the

Table 3 Direct shear and compressive strengths of specimens

Author	ID	f'_c MPa	V_f %	l_f/d_f	τ_{cr} MPa	τ_{max} MPa	τ_{n120} MPa	τ_{n100} MPa	τ_{n80} MPa
This study	Z-0.41-1	52.7	0.41	65	2.9	3.6	2.3	2.1	1.9
	Z-0.74-2	52.6	0.74		3.7	4.4	2.5	2.3	2.1
	FIP-0.41-1	52.7	0.41		4.4	4.3	3.4	2.7	1.7
	FIP-0.41-2	52.7	0.41		3.7	5.1	1.2	1.0	0.8
	FIP-0.74-1	52.6	0.74		4.5	4.4	3.6	2.7	1.8
	FIP-0.74-2	52.6	0.74		3.3	4.6	3.4	–	–
	JSCE-PC-1	47.3	0.00		2.9	–	–	–	–
	JSCE-PC-2	47.3	0.00		3.8	–	–	–	–
	JSCE-0.41-1	52.7	0.41		3.6	3.7	1.4	1.3	1.3
	JSCE-0.41-2	52.7	0.41		3.4	3.8	3.1	2.8	2.5
	JSCE-0.74-1	52.6	0.74		5.0	5.9	3.7	3.6	3.6
	JSCE-0.74-2	52.6	0.74		5.7	5.4	2.3	1.7	1.5
Araujo et al. [11]	Ar-JSCE-0-1	51.8	0.00	65	4.1	–	–	–	–
	Ar-JSCE-1-1	65.3	1.00		3.1	8.6	7.4	5.3	3.8
	Ar-JSCE-2-1	71.3	2.00		3.5	9.5	9.3	8.8	7.3
Barragán et al. [3]	Ba-Z-0.00-1	40.2	0.00	80	5.2	5.2	–	–	–
	Ba-Z-0.25-1	38.9	0.25		6.1	6.2	2.1	1.4	–
	Ba-Z-0.5-1	38.3	0.50		6.0	5.9	3.3	3.0	3.0
	Ba-Z-0.00-2	77.7	0.00		5.5	5.5	–	–	–
	Ba-Z-0.25-2	76.5	0.25		5.0	8.2	4.7	4.1	4.0
	Ba-Z-0.5-2	77.8	0.50		8.2	10.0	5.4	5.0	4.7
Mostafazadeh and Abolmaali [24]	Mo-JSCE-0-1	28.3	0.00	65	4.2	–	–	–	–
	Mo-JSCE-0.25-1	31.3	0.25		4.7	–	2.6	2.1	1.6
	Mo-JSCE-0.52-1	33.0	0.52		5.0	–	3.1	2.8	2.6
	Mo-JSCE-0.78-1	32.8	0.78		5.6	–	3.5	3.2	2.4
	Mo-JSCE-1.00-1	31.1	1.00		6.0	–	4.7	4.3	3.8
	Mo-JSCE-0-2	34.0	0.00		5.5	–	0.8	0.8	–
	Mo-JSCE-0.25-2	39.4	0.25		6.3	–	3.6	3.3	3.0
	Mo-JSCE-0.52-2	39.9	0.52		6.8	–	5.0	4.8	4.0
	Mo-JSCE-0.78-2	39.8	0.78		7.4	–	5.4	5.1	4.3
	Mo-JSCE-1.00-2	38.3	1.00		7.9	–	5.7	5.3	5.1

- The value is not reported

Fig. 7 Typical failure modes of beams tested under bending: **a** PC, **b** D_f = 32.0 kg/m^3, **c** D_f = 58.1 kg/m^3

beams occurs inside the middle third of the span as requested by ASTM C-1609 standard [12]. Table 4 summarizes the values of bending tensile strength and compressive strength of specimens in this study and those reported by other studies available in the literature, where f_{cr} is the flexural-tensile strength at first cracking, f_{max} is the maximum flexural-tensile strength, and $f_{L/600}$, $f_{L/300}$ and $f_{L/150}$ are residual flexural-tensile strengths for mid-span deflections of $L/600$, $L/300$ and $L/150$, respectively. Data from the bending test of PC and from one specimen with V_f of 0.41% in this study were not included in the table,

Table 4 Flexural tensile strength and compressive strength of specimens

Autor	f'_c MPa	V_f %	f_{cr} MPa	f_{max} MPa	$f_{L/600}$ MPa	$f_{L/300}$ MPa	$f_{L/150}$ MPa
This study	52.7	0.41	6.77	7.20	6.76	7.20	5.79
	52.6	0.74	6.32	8.19	7.48	8.00	7.97
	52.6	0.74	6.86	7.41	7.28	7.04	5.71
Araujo et al. [11]	51.8	0.00	–	–	–	–	–
	65.3	1.00	2.60	2.70	0.77	0.48	0.34
	71.3	2.00	4.02	4.15	2.31	1.16	0.77
Barragán et al. [3]	40.2	0.00	1.60	1.62	–	–	–
	38.9	0.25	1.73	1.76	0.97	1.07	–
	38.3	0.50	1.93	1.94	2.08	2.23	–
	77.7	0.00	1.95	–	–	–	–
	76.5	0.25	1.93	2.8	2.71	2.73	–
	77.8	0.50	2.40	4.8	4.67	4.71	–
Mostafazadeh and Abolmaali [26]	28.3	0.00	–	3.33	0.13	–	–
	31.3	0.25	–	3.57	0.68	0.73	0.67
	33.0	0.52	–	4.00	1.47	1.83	1.37
	32.8	0.78	–	4.01	3.27	3.31	3.08
	31.1	1.00	–	3.96	3.68	3.87	3.07
	34.0	0.00	–	3.60	–	–	–
	39.4	0.25	–	4.27	0.80	0.93	0.67
	39.9	0.52	–	4.53	1.87	1.79	1.31
	39.8	0.78	–	4.49	2.87	3.28	2.85
	38.3	1.00	–	4.47	3.81	3.96	2.77

- The value is not reported

because beam instrumentation did not work adequately during those tests.

3.5 Correlation Between Flexural-Tensile and Direct Shear Stresses

To facilitate estimation of the direct shear stress of SFRC from the results of the widely used four-point bending test (4PBT), a model to correlate the direct shear stress of SFRC associated with τ_{cr}, τ_{n120}, τ_{n100}, τ_{n80} and the flexural-tensile stress of SFRC associated to f_{cr}, f_{L600}, f_{L300} and f_{L150} is developed in this section. An analysis of variance (ANOVA) was carried out to identify the variables that significantly influence the correlation between direct shear and flexural-tensile stresses. The variables studied in the ANOVA were the compressive strength of SFRC (f'_c), reinforcement index ($RI = V_f \times l_f/d_f$), and number of shear planes of the test specimen (N_p). The ANOVA compares the difference of the variance generated by the studied variable and the intrinsic variance of the data to evaluate the influence of the studied variable (independent variable) on the intrinsic or dependent variables. Identification of independent variables that significantly influence the correlation between shear and flexural-tensile stresses was carried out by means of an ANOVA. In this study, the dependent variables are τ_{cr}, τ_{max}, τ_{n120}, τ_{n100}, τ_{n80}, f_{cr}, f_{max}, f_{L600}, f_{L300} and f_{L150}. Those variables were correlated with the independent variables: f'_c, RI and N_p.

The ANOVA analysis establishes the characteristic value of Fisher's distribution (F) and compares it to the critical value of F of the independent variables. The value of F was calculated for each independent variable and residual strength, and then the critical value of F (F_{crit}) was calculated. The value of F_{crit} was equal to 3.68 and it was calculated from Fisher's distribution with a significance level of 5%. In Fig. 8, F_{crit} is represented by a continuous horizontal red line. The variables with $F > F_{crit}$ indicate that they influence both flexural-tensile and direct shear strengths. Figure 8 shows the ANOVA to determine the incidence of f'_c, RI and N_p on the shear and flexural-tensile stresses of SFRC. The results of the ANOVA analysis in Fig. 8 showed that the variable with more influence on the

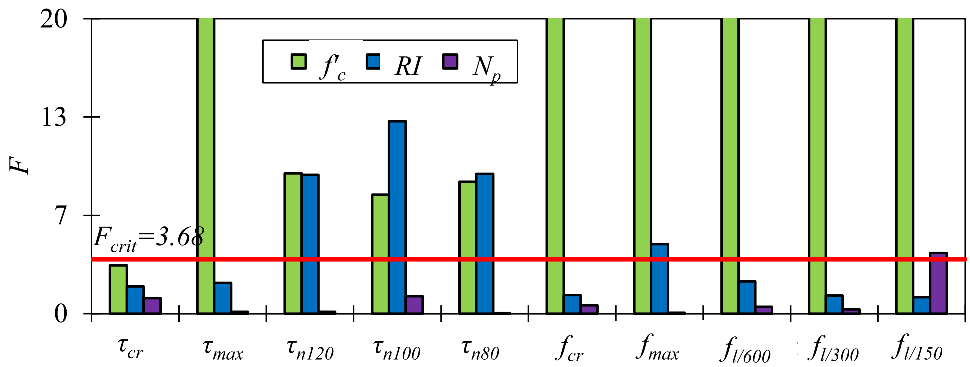

Fig. 8 ANOVA

shear and flexural-tensile stress values of SFRC was f'_c. The statistical results shown in Fig. 8 suggest that the Reinforcement Index ($RI = V_f \times l_f/d_f$) affects post-cracking shear and flexural-tensile stresses of SFRC. The ANOVA results also demonstrated that, except for the flexural-tensile stress f_{L150}, the effect of the N_p factor is lower than the effect of f'_c and RI on direct shear and flexural-tensile stresses.

Sarbini et al. [2] used the results of bending test on 150 mm × 150 mm × 750 mm beams to develop equations to predict the shear stress of beams reinforced with steel bars and steel fibers. These authors identified the critical state where steel fibers still develop additional tension to increase the direct shear strength of SFRC. In the present study, the correlation between direct shear stress and flexural-tensile stress of SFRC was performed from a database including the results obtained during direct shear tests (see Table 3) and during the bending test (see Table 4) of this study and of those reported by Barragán et al. [6], Araújo et al. [11], and Mostafazadeh and Abolmaali [26].

Figure 9 shows the values of direct shear strength at limit states of cracking, maximum strength and residual strengths (τ_{n120}, τ_{n100}, τ_{n80}), and the flexural-tensile strengths (f_{cr}, f_{max}, f_{L600}, f_{L300}, f_{L150}) of SFRC tested in this study and those reported in the literature [6, 11, 26]. Based on ANOVA results, the parameters f'_c, RI and N_p were used to normalize direct shear and flexural-tensile stresses of studies reported by different authors with different material strengths, fiber dosages and types of fibers. For the cracking limit state, the data of PC and SFRC in Fig. 9a were normalized exclusively with f'_c since this limit state is the onset of the main effect of the fibers on performance of SFRC. For limit states of maximum strength and residual strengths, Fig. 9b–e show that f'_c, RI and N_p were used to normalize post-cracking shear and flexural-tensile stresses. From the trends in Fig. 9, Eq. (3) is proposed in this study to estimate direct shear strengths of SFRC (τ_{cr}, τ_{max}, τ_{n120}, τ_{n100}, τ_{n80}) as a function of flexural-tensile strengths (f_{cr}, f_{max}, f_{L600}, f_{L300}, f_{L150}). The variables H and M, and the constant K are used in Eq. (3), where H represents the ratios of shear strengths $\tau_{cr}/\sqrt{f'_c}$, $\tau_{max}/(\sqrt{f'_c} \times N_p \times RI)$, $\tau_{n120}/(\sqrt{f'_c} \times N_p \times RI)$, $\tau_{n100}/(\sqrt{f'_c} \times N_p \times RI)$, $\tau_{n80}/(\sqrt{f'_c} \times N_p \times RI)$, M corresponds to the ratios of flexural-tensile strengths $f_{cr}/\sqrt{f'_c}$, $f_{max}/(\sqrt{f'_c} \times RI)$, $f_{L600}/(\sqrt{f'_c} \times RI)$, $f_{L300}/(\sqrt{f'_c} \times RI)$, $f_{L150}/(\sqrt{f'_c} \times RI)$, respectively, and K corresponds to the constant of the trend, which corresponds to the slope of the line between the data of direct shear strengths and flexural-tensile strengths. Table 5 summarizes the values of the variables H and M, and the constants K included in Eq. (3).

$$\mathrm{H} = \mathrm{K} \times \mathrm{M} \tag{3}$$

Figure 9a shows that the results of direct shear and flexural-tensile strengths at limit states of cracking and maximum strength (τ_{cr} and f_{cr}) measured in this study are in line with the trend of the values reported by Araújo et al. [11]. The values of f_{cr} and f_{max} measured in this study, however, are not in line with the trend of the data reported by Barragán et al. [6], since the values of f_{cr} and f_{max} reported by these authors ranged from 1.6 to 4.6 MPa, which are significantly lower than the results obtained in this study (6.3 MPa a 7.4 MPa). The values of $f_{L/600}$, $f_{L/300}$, and $f_{L/150}$ measured in this study are not in line with the trend of the data reported by Mostafazadeh and Abolmaali [26], since the values reported by these authors ranged from 0.13–4.5 MPa, which are lower than the values obtained in this study (close to 7.03 MPa).

4 Conclusions

Measured results in the study aided to identify that compressive strength of SFRC was 11.4% (52.7 MPa/47.3 MPa) and 11.2% (52.6 MPa/47.3 MPa) higher than that of PC when increasing V_f from 0.41 to 0.74%, respectively. In terms of bending tests, the results of the study showed that, as previously reported by other studies,

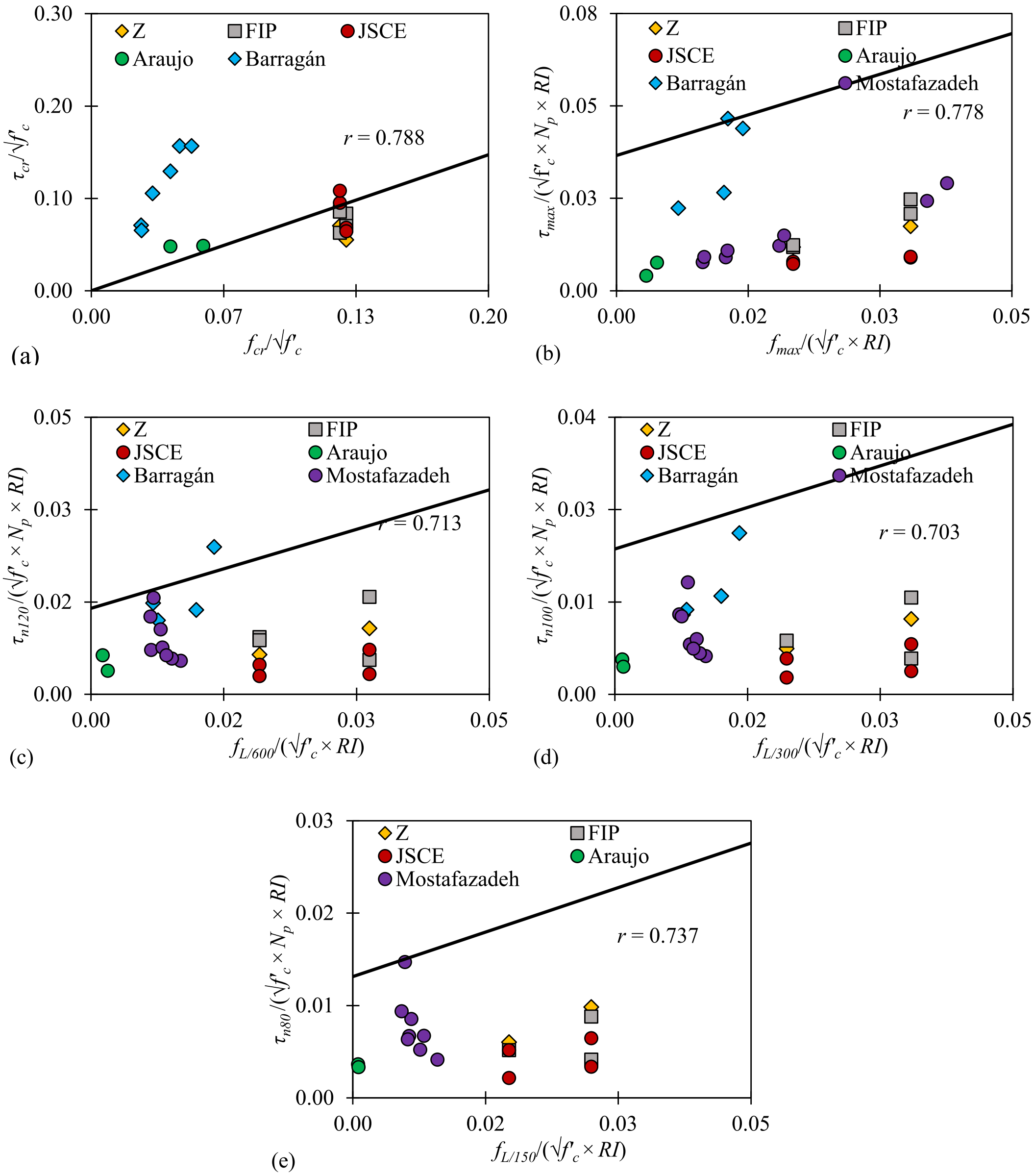

Fig. 9 Direct shear strengths as a function of flexural-tensile strengths (units in MPa): **a** τ_{cr}–f_{cr}, **b** τ_{max}–f_{max}, **c** τ_{n120}–$f_{L/600}$, **d** τ_{n100}–$f_{L/300}$, **e** τ_{n80}–$f_{L/150}$

Table 5 Variables of Eq. (3) (units in MPa)

H	K	M
$\tau_{cr}/\sqrt{f'_c}$	0.736	$f_{cr}/\sqrt{f'_c}$
$\tau_{max}/(\sqrt{f'_c} \times N_p \times RI)$	0.664	$f_{max}/(\sqrt{f'_c} \times RI)$
$\tau_{n120}/(\sqrt{f'_c} \times N_p \times RI)$	0.412	$f_{L/600}/(\sqrt{f'_c} \times RI)$
$\tau_{n100}/(\sqrt{f'_c} \times N_p \times RI)$	0.339	$f_{L/300}/(\sqrt{f'_c} \times RI)$
$\tau_{n80}/(\sqrt{f'_c} \times N_p \times RI)$	0.276	$f_{L/150}/(\sqrt{f'_c} \times RI)$

flexural-tensile cracking strength does not vary significantly by increasing the content of steel fibers. Maximum flexural-tensile strength of SFRC in this study and other studies reported in the literature increased proportionally with the content of steel fibers; for instance, f_{max} of SFRC beams with V_f of 0.76% was 8.3% higher than that of beams with V_f of 0.38%.

Shear test results showed the significant effects of steel fibers on shear strength of SFRC. The maximum shear strength (τ_{max}) of SFRC with V_f of 0.76% obtained using the JSCE-SF6 method was 50.6% (5.65 MPa/3.75 MPa) higher than that of SFRC with V_f of 0.38%. The τ_{max} of SFRC obtained using the Z-type method exhibited a similar behavior to that observed when using the JSCE-SF6 tests. The shear strength of SFRC with 0.76% obtained using the Z-type method was 22% higher than that of SFRC with V_f

of 0.38%. The contribution of steel fibers to residual shear strength of concrete allows greater displacements due to the suitable adherence of fiber to concrete.

A numerical correlation was also proposed to estimate the direct shear and flexural-tensile properties of SFRC in beams and columns at the limit states of first cracking, maximum strength and residual strengths. According to the results of the analysis of variance (ANOVA), the parameters f'_c, RI and N_p were included in the equations of correlation between direct shear and flexural-tensile strengths. The variables RI and N_p affect residual shear strengths (τ_{n120}, τ_{n100}, τ_{n80}), since the effect of steel fibers on performance of concrete is mainly observed after cracking. Variable f'_c had the most significant influence on all dependent variables (f_{cr}, f_{max}, f_{L600} f_{L300} f_{L150}, τ_{cr}, τ_{max}, τ_{n120}, τ_{n100} and τ_{n80}) in this study. The numerical correlation was planned using simple variables of shear and flexural-tensile strengths at first cracking, maximum and residual strengths, which can be easily implemented in building codes. The correlation model developed is practical for code-compliant design purposes since the direct shear performance of SFRC can be estimated from the results of the commonly used bending test. The equations proposed in this study can be used to calculate the average mechanical properties of SFRC that comply with the following characteristics: normal-weight concrete, compressive strength of concrete ranging from 28 to 75 MPa, with V_f from 0.3 to 2.0%, and with l_f/d_f of steel fibers ranging from 65 to 80. The results of this study would stimulate the use of SFRC in code-based design because the proposed correlation aids to estimate direct shear performance from the results of a widely used bending test.

Acknowledgements The authors would like to acknowledge *Vicerrectoría de Investigaciones* of the UMNG for the financial support through Project EXT-ING-4074. The authors also gratefully acknowledge the support of Argos-Colombia and Dramix-Proalco for donating the materials used in the experimental program of this study, and to USI Library of Institute of Engineering at UNAM for providing some of the references. The authors also would like to thank Research Assistant Eyli Salcedo at Universidad Militar Nueva Granada (UMNG) for data and figure processing. The views expressed in this paper are solely those of the authors and do not necessarily reflect the views of the sponsors.

Funding Open Access funding provided by Colombia Consortium.

Data availability statement Some or all data, models, or code that support the findings of this study are available from the corresponding author upon reasonable request.

Declarations

Conflict of interest The authors declare no competing interest to declare that are relevant to the content of this article.

References

1. López J (2015) Analysis of properties of concrete reinforced with short steel fibers and polypropylene macro-fibers: influence of type and content of fibers. Msc Thesis, National University of Mexico, UNAM **(in Spanish)**
2. Sarbini N, Ibrahim I, Saim A, Kadir M, Mohsin S (2016) Development of shear stress equation contributed by steel fibre reinforced concrete. ARPN J Eng Appl Sci 11(8):5445–5450
3. Lozano C (2012) Use of steel fiber reinforced concrete deep beams. Bch Thesis, National University of Mexico, UNAM **(in Spanish)**
4. Sarta H, Silva J (2017) Comparative analyses between plain concrete and concrete reinforced with 4% and 6% of steel fibers. Bch Thesis, Catholic University of Colombia **(in Spanish)**
5. Marmol P (2010) Concrete with steel fibers: mechanical characteristics. MSc Thesis, Universidad Politécnica de Madrid, Spain **(in Spanish)**
6. Barragán B, Gettu R, Agulló L, Zerbino R (2006) Shear failure of steel fiber-reinforced concrete based on push-off tests. ACI Mater 103(4):251–257. https://doi.org/10.14359/16608
7. Wu P, Wu C, Liu Z, Hao H (2019) Investigation of shear performance of UHPC by direct shear tests. Eng Struct 183:780–790. https://doi.org/10.1016/j.engstruct.2019.01.055
8. ACI Committee 318 (2019) Building code requirements for structural concrete. American Concrete Institute, Farmington Hill, MI
9. Martin L, Perry C (2008) PCI design handbook: precast and prestressed concrete. American Concrete Institute, Farmington Hills, MI, vol 1
10. Khanlou A, MacRae G, Scott A, Hicks S, Clifton G (2012) Shear performance of steel fibre- reinforced concrete. In: Proceedings of Australasian structural engineering conference, Christchurch, New Zealand
11. Araújo D, Nunes T, Días R, Andrade M (2014) Shear strength of steel fiber reinforced concrete. Acta Scientiarum 36(3):389–397. https://doi.org/10.5335/rsee.v9i2.2612
12. Carrillo J, Vargas J, Arroyo O (2021) Correlation between flexural-tensile performance of concrete reinforced with hooked-end steel fibers using American and European standards. Mater Civ Eng 33(8):04021211. https://doi.org/10.1061/(ASCE)MT.1943-5533.0003840
13. Carrillo J, Torres D, Guerrero H (2021) Correlation between results obtained from four-point bending tests (4PBT) and double punch tests (DPT) in concrete reinforced with hooked-end steel fibers. Eng Struct 239:1–12. https://doi.org/10.1016/j.engstruct.2021.112353
14. JSCE-SF (1990) Method of tests for shear strength of steel fiber reinforced concrete. Japan Society of Civil Engineers, JSCE, Tokyo, pp 67–69

15. FIP (1978) Shear at the interface of precast and in-situ concrete. Lausanne: guide to good practice. Technical report, The International Federation for Structural Concrete (fib)
16. ASTM C-1609 (2012) Standard test method for flexural performance of fiber-reinforced concrete (using beam with third-point loading). American Society for Testing and Materials, ASTM
17. ASTM C-39 (2021) Standard test method for compressive strength of cylindrical concrete specimens. American Society of Testing Materials, ASTM
18. UNE-EN 14488 (2007) Testing sprayed concrete—Part 7: fiber content of fiber reinforced concrete." European Committee for Standardization, CEN, Belgium
19. Carmona S, Cabrera M (2009) Shear behavior of Steel fiber reinforced concrete". Ingeniería de Construcción 24(1):79–94. https://doi.org/10.4067/S0718-50732009000100004
20. Higashiyama H, Banthia N (2008) Correlating flexural and shear toughness of lightweight fiber-reinforced concrete. ACI Materials 105(3):251–257. https://doi.org/10.14359/19821
21. Markovich I, Van Mier J, Walraven J (2001) Single fiber pullout from hybrid fiber reinforced concrete. HERON 46(3):191–200
22. Mattock A, Johal L, Chow H (1975) Shear transfer in reinforced concrete with moment or tension acting across the shear plane. PCI J 20(4):66–13. https://doi.org/10.15554/pcij.07011975.76.93
23. Yoo D, Kim S, Park J (2017) Comparative flexural behavior of ultra-high performance concrete reinforced with hybrid straight steel fibers. Constr Build Mater 132:219–229. https://doi.org/10.1016/j.conbuildmat.2016.11.104
24. Gao D, Zhang L, Nokken M (2017) Mechanical behavior of recycled coarse aggregate concrete reinforced with steel fibers under direct shear. Cem Concr Compos 79:1–8. https://doi.org/10.1016/j.cemconcomp.2017.01.006
25. Carrillo J, Salcedo E, Rojas F (2023) Evaluating direct shear performance of steel fiber-reinforced concrete. Mater Civ Eng 36(2):04023559. https://doi.org/10.1061/JMCEE7.MTENG-165
26. Mostafazadeh M, Abolmaali A (2016) Shear behavior of synthetic fiber. PhD Thesis, University of Texas, Arlington